Poly(vinyl chloride)/Metallic Oxides/Organically Modified Montmorillonite Nanocomposites: Preparation, Morphological Characterization, and Modeling of the Mechanical Properties

Antonio Rodolfo, Jr.,[1,2] Lucia Helena Innocentini-Mei[2]

[1]*Braskem S/A, Polymers Business Unit, Avenida das Nações Unidas, 8501, 23rd floor, CEP 05425-070, São Paulo, SP, Brazil*
[2]*Department of Polymer Technology, School of Chemical Engineering, State University of Campinas, P. O. Box 6066, CEP 13083-970, Campinas, SP, Brazil*

Received 4 July 2009; accepted 14 September 2009
DOI 10.1002/app.31442
Published online 1 December 2009 in Wiley InterScience (www.interscience.wiley.com).

ABSTRACT: Poly(vinyl chloride), metallic oxides (from copper, molybdenum, and zinc), and organically modified montmorillonite (O-MMT) nanocomposites were prepared in a melt-blending or intercalation-in-the-molten-state process. The morphology of the nanocomposites was evaluated with X-ray diffraction (XRD) and transmission electron microscopy (TEM). Properties, such as the mechanical, thermal, and electrical properties, and the dynamic thermal stability against dehydrochlorination were also evaluated. Nanocomposites with a hybrid intercalated/exfoliated structure were obtained in all of the situations considered, as demonstrated by the XRD and TEM results and indirectly by the increment of Young's modulus of the formulations with increasing amount of O-MMT incorporated. The modeling of Young's modulus by the Halpin–Tsai, Hui–Shia, and Lewis–Nielsen theories showed that the process of nanocomposite preparation allowed the aspect ratio of the clay particles to increase; these values were comparable to those nanocomposites obtained by other researchers with different polymeric matrices and methodologies. © 2009 Wiley Periodicals, Inc. J Appl Polym Sci 116: 422–432, 2010

Key words: clay; mechanical properties; microstructure; nanocomposites; poly(vinyl chloride) (PVC)

INTRODUCTION

Poly(vinyl chloride) (PVC) is the second most consumed thermoplastic in the world, with a global resin demand of over 33 million tons in 2008. The worldwide PVC resin production capacity is estimated to be around 43 million tons per year.[1] In 2008, Brazil was responsible for the consumption of approximately 1 million tons, or 2.7% of the worldwide PVC resin demand. These data show the potential growth of the demand for such resins in Brazil, as the per capita consumption, around 5 kg/person/year, is still low compared with other countries.

PVC may be considered one of the most versatile polymers. As the resin is formulated through the incorporation of additives, the features of PVC can be changed in a wide spectrum of properties according to the final application, ranging between rigid and extremely flexible states. This wide range of properties allows for the use of PVC in applications that range from pipes and rigid profiles to civil construction to toys and flexible laminates for the storage of blood and plasma. The wide versatility of PVC is also partly due to its adequacy to the most varied molding processes, and it can be injected, extruded, rotomolded, and spread-coated, among many other processing alternatives.

Polymer nanocomposites are part of a new class of composites containing small amounts, usually below 5 wt %, of nanoparticles for reinforcement; these nanoparticles are usually between 1 and 100 nm in one of their dimensions.[2,3] Because of their nature, the particles can be in the zero-dimensional (nanoparticles), one-dimensional (nanofibers), or two-dimensional (nanoplatelets) scales, depending on the number of dimensions in the nanoscale.[4]

Over recent decades, there has been growing interest in the field of polymer nanocomposites, following the development of nanotechnology, thanks to its special features. They allow for the attainment of properties that are equivalent to those of traditional composites and also have unique optical, electrical, and magnetic properties.[5–7]

Correspondence to: A. Rodolfo, Jr.. (antonio.rodolfo@braskem.com.br).

Contract grant sponsors: Braskem S/A through the Núcleo de Estudos Orientados do PVC (NEO PVC) Program.

Polymer nanocomposites with high-aspect-ratio particles present better mechanical and thermal properties than conventional composites, even with a lower reinforcement content, because of the larger area of contact between the polymer matrix and the dispersed phase. The presence of nanoclay provides important barrier properties, in most cases, low permeability, better chemical resistance, and better flame retardance, which depend on the ability to individually disperse these particles in the polymer matrix.[8,9]

Clays are minerals with a chemical constitution that allows for the separation of silicate layers (exfoliation) with the consequent possibility of polymer chain intercalation. The fact that they have a high superficial area makes clays bring a series of potential benefits to polymer materials, including PVC, that is, greater rigidity and mechanical resistance, better toughness, a greater barrier against the diffusion of gases, lower permeability, higher distortion and softening temperatures, lower flammability, better chemical resistance, and greater dimensional stability.[10–14]

An exchange of interlayer cations by quaternary ammonium salts generates an organophilic clay and reduces the surface energy of the clay layers. This allows the diffusion and penetration of organic species between the layers and eventually separates or exfoliates them. In the particular case of PVC, nevertheless, the bigger problem arising from the use of quaternary ammonium salts is related to its high Lewis acid character. This effect is highly harmful for the polymer and promotes fast thermal degradation through the dehydrochlorination mechanism. Such an undesirable fact cannot be ignored in the production PVC nanocomposites with organically modified clays.[15]

The larger concentration of published studies regarding PVC-based nanocomposites have focused on the intercalation of clays, especially montmorillonite (MMT).[16–25] Articles relating to intercalation or mixture processes in the molten state have also been more frequent. That is understandable, under the experimental point of view, as the polymerization of vinyl chloride, which is a gas at room temperature and pressure, is complex from a practical point of view. Such a fact has been responsible for the reduced number of academic laboratories working in this field, particularly because of the toxicity factor of the monomer. On the other hand, intercalation or mixture processes in the molten state require simple, more affordable equipment, such as extruders, torque rheometers, or two-roll mills. This process does not demand as much concern as the polymerization process, which is not always available to all research groups.

Our purpose in this work was to develop PVC nanocomposites in the presence of organically modified clay and Cu(II), Mo, and Zn oxides, which were incorporated to the nanocomposites for the evaluation of their effects on the basic properties of the material and so that we could study the combustion and smoke suppression in a future step. The formation of the nanocomposites was evaluated via complementary techniques such as X-ray diffraction (XRD) and transmission electron microscopy (TEM). The Young's modulus resulting from the prepared formulations were modeled with mechanical reinforcement theories developed by Halpin–Tsai, Hui–Shia, and Lewis–Nielsen; we allowed for comparison between the experimental and theoretical results and for inferences on the intercalation/exfoliation state in each case studied.

TABLE I
PVC Compound Formulation Used in This Study

Component	Amount (phr)
Norvic SP 1000 (PVC resin K 65)	100
Naftomix XC-1202 (Ca/Zn thermal stabilizer)	3.5
DIDP	45
Drapex 6.8 (ESO)	5
Barralev C (precipitated calcium carbonate)	40
Stearic acid	0.2

EXPERIMENTAL

Materials

The formulation of the PVC compound, taken as a reference and summarized in Table I, was based on common practices used in PVC cable transformers in Brazil. PVC resin, with a K value of 65 $\pm$ 1 (Norvic SP 1000, Braskem S/A, Camaçari, Brazil), was used as the polymer matrix. The other components of the basic formulation are detailed in Table I and were acquired from commercial sources.

The clay used in this study was Cloisite 30B, supplied by Southern Clay Products, Inc. (Gonzales, TX), which has been widely used in other studies involving PVC nanocomposites.[16,18–23] It is a natural MMT, modified with a methyl-2-hydroxyethyl based quaternary ammonium salt, coupled to a fatty chain of animal origin (tallow), with approximately 65% C_{18}, 30% C_{16} and 5% C_{14}.[26] This clay has, as a reference, an interlayer spacing value (d_{001}) of 1.85 nm (XRD) and was incorporated in 2.5 and 5 wt % dosages.

A goal of these studies was to obtain PVC composites with a lower emission of smoke during combustion. For this, some of the evaluated formulations received a 5 or 10 wt % addition of a 1 : 1 : 1 CuO/MoO_3/ZnO mixture. Table II provides full details of the formulations evaluated in this study.

TABLE II
Complete Description of the PVC Formulations Evaluated in This Study

Identification	PVC base compound (%)	Metallic oxides (%)	O-MMT (%)
PVC-0-0	100	0	0
PVC-0-2.5	97.5	0	2.5
PVC-0-5	95	0	5
PVC-5-0	95	5	0
PVC-5-2.5	92.5	5	2.5
PVC-5-5	90	5	5
PVC-10-0	90	10	0
PVC-10-2.5	87.5	10	2.5
PVC-10-5	85	10	5

Preparation of the nanocomposites

Where applicable, the clay was preexfoliated in a hot diisodecylphtalate (DIDP)/epoxidized soybean oil (ESO) mixture, according to the procedure described in ref. 21. In this process, the amount of plasticizers needed for each formulation was heated at 90–100°C in a beaker over a heating plate. The clay needed for the formulation was then submitted to shear in the presence of the plasticizers through a Fisatom 7137 (70 W) intensive mixer (São Paulo, Brazil) at 1200–1300 rpm for 20 min.

All formulations were homogenized through a Mecanoplast ML-9 intensive mixer (Rio Claro, Brazil). Initially, the resin, thermal stabilizer, calcium carbonate, stearic acid, and where applicable, metallic oxides were added to the mixer at room temperature, and after being submitted to shear up to 80°C, the plasticizers DIDP and ESO were incorporated, along with the preintercalated/exfoliated clay. The final composition was discharged at 110°C; this was followed by cooling at 35–40°C to prevent the formation of agglomerates.

The formulations were then processed in a Miotto LM 03/30 single-screw extruder (30 mm, length/diameter = 25) (São Bernardo do Campo, Brazil), through the temperature profile 140–145–150°C at 80 rpm. Test specimens were obtained from the pellets in a Mecanoplast laboratory two-roll mill. The temperature, processing time, and rotation to prepare the 3 mm thick plates from which the test specimens were taken were 160°C, 3 min, and 20 rpm, respectively. Pressing was performed between stainless steel plates in a Luxor (São Paulo, Brazil) press at 175°C.

Morphological evaluation of the nanocomposites

The morphology of the nanocomposites was evaluated with two complementary techniques:[12,13] XRD and TEM. X-ray diffractograms were obtained from pressed samples in a Siemens (Karlsruhe, Germany) D500 diffractometer in the reflection mode through an X-ray beam of Cu Kα (λ = 1.54 Å). Scans were performed from $2\theta = 1$ to 45° with a 0.05° step.

Thin samples (ca. 70 nm thick) of each formulation were obtained in a Leica (Wetzlar, Germany) EM FC6 ultramicrotome with a Drukker 3 mm/45° diamond blade at −140°C. The TEM observations of these thin samples were performed in a JEOL (Tokyo, Japan) JEM-1200 EX II TEM instrument at 80 kV.

Mechanical properties

The tension properties (Young's modulus, stress, and elongation at break) were determined in 10 ASTM D 638-08 type IV test specimens for each formulation in an Alliance 5/RT MTS universal testing machine (Eden Prairie, MN) at 50 mm/min. The tests were carried out at 23 ± 2°C.

Specific weight

The specific weight of the samples was determined via the hydrostatic weighing method on an analytical balance with 0.0001 g of accuracy at 23 ± 2°C.

Thermal properties

The dynamic mechanical analysis (DMA) of the samples was performed in a Q800 TA Instrument (New Castle, DE) in the cantilever mode at a frequency of 1 Hz. The samples were scanned from −150 to 150°C at a rate of 2°C/min.

Electrical properties

The volumetric electrical resistivity (VER) of the samples was evaluated in an Agilent 4339B high-resistance meter (Santa Clara, CA) equipped with a 16008B resistivity cell, according to ASTM D 257-07. Three test specimens of each formulation were evaluated at 23 ± 2°C after conditioning for 40 h in distilled water.

Dynamic thermal stability

The dynamic thermal stability (under shear) of the composites was evaluated in a torque rheometer from Thermo Haake Polylab System (model Rheocord 300p) (Karlsruhe, Germany) equipped with a Rheomix 610P mixer and roller rotors and Polyview 2.1.1 software. The tests were carried out in duplicate according to ASTM D 2538-02 at 200°C, 90 rpm, and 62 g.

Statistical analysis

Statistical analyses and the modeling of the Young's modulus data through the least-squares method were performed via Microsoft Excel. More sophisticated analyses, such as the evaluation of the effects of the different variables studied in this experimental project [content of metallic oxides and organically modified montmorillonite (O-MMT)], were carried out with Minitab 15 (Minitab, Inc., State College, PA) and

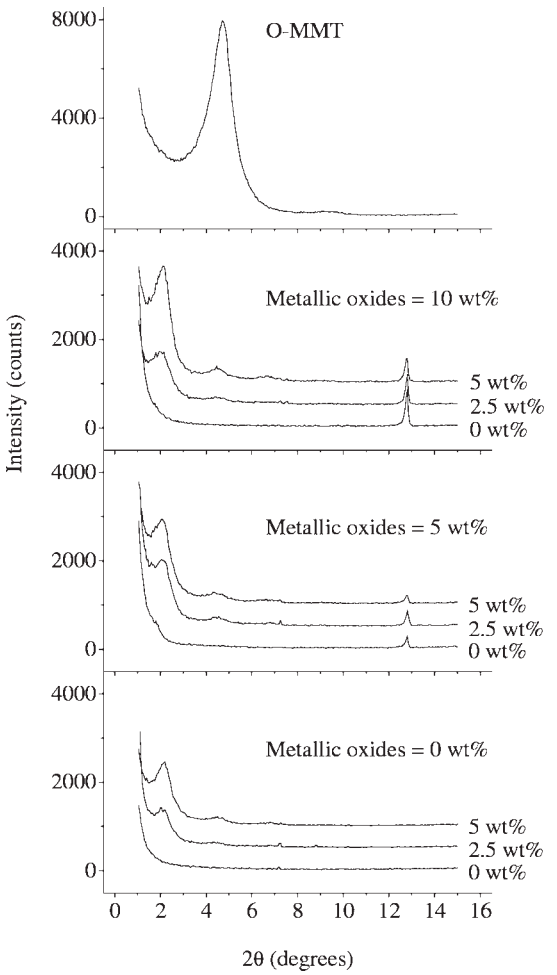

Figure 1 XRD diffractograms for PVC/metallic oxides/O-MMT nanocomposites as a function of the $CuO/MoO_3/ZnO$ content.

Design-Expert 7.1 (StatEase, Inc., Minneapolis, MN), as the formulations evaluated corresponded to a three levels by two factors design of experiments.

RESULTS AND DISCUSSION

Morphological evaluation of the nanocomposites

Figure 1 presents the XRD results of the studied formulations, which put in evidence the formation of hybrid intercalated/partially exfoliated PVC/O-MMT nanocomposites. In all cases, there was a dislocation and attenuation of the d_{001} peak of the O-MMT, originally at $2\theta = 4.70^\circ$ ($d_{001} = 1.88$ nm, in accordance with the supplier's data[26]) for values at $2\theta = 2.05$–2.20° ($d_{001} = 4.01$–4.30 nm). This dislocation of the main diffraction peak of O-MMT for lower 2θ angle values was an important indication of the increase in the spacing between the silicate lamellae, which resulted from the intercalation of plasticizer molecules and/or PVC chains in the clay galleries. Results obtained by other authors,[16,18–25] with bis(2-ethylhexyl)phthalate (DEHP or DOP) and DIDP as plasticizers, indicated several values for d_{001}, ranging between 3.1 and 4.9 nm, that is, in the same magnitude of the results found here, which corroborated these studies.

The gelation and fusion of PVC grains during processing is a quite complex phenomenon because of its kinetics and has been widely studied.[27–31] In short, it is the destruction of the PVC grains (120–150 μm in diameter), originating from the suspension polymerization process, due to shear, with the formation of the gel's primary particles ($\sim$ 1 μm in diameter), fused by the interdiffusion of macromolecules caused by shear and temperature. In this context, we believe that the intercalation of PVC molecules in silicate galleries is not very efficient because the intercalation of organic low-molecular-weight molecules, such as the plasticizer, would be more favorable thermodynamically; this would have promoted the observed increase in the interlayer spacing identified in the XRD measures.

The presented diffractograms also suggest that, even after processing, there was still evidence of the presence of tactoids (nonexfoliated agglomerates) remaining from the intercalation/exfoliation of the O-MMT, as demonstrated by the presence of quite discreet, wide peaks around $2\theta = 4.70^\circ$. The examination of the TEM images presented in Figures 2 and 3 provided evidence for the presence of exfoliated silicate sheets in all of the samples coexisting with intercalated structures and even some tactoids; this confirmed the results found in the XRD analysis. Larger particles, characteristic of calcium carbonate and metallic oxides species, were also seen in the examination of the TEM images. The same pattern was observed in all of the studied situations, independently of the metallic oxide content in the sample under observation.

Paul and Robeson[12] mentioned that such coexistence of different levels of exfoliation, from completely nonexfoliated (tactoids) to total exfoliated silicate lamellae dispersed in the polymer matrix, is common in nanocomposites obtained via the intercalation process by melt blending. It occurs because of the mechanism of dispersion and exfoliation of the clay. A mechanism proposed by Fornes et al.[32] suggests that the process of exfoliation of the clay is initiated by the formation of tactoids by the original O-MMT particles. Such agglomerates are later deformed due to shear during processing in the molten state. Then, because of a combined process of diffusion of chains and other organic components, such as the plasticizers, and the resulting shear, the silicate sheets or lamellae become intercalated in their galleries and may achieve full exfoliation.

Mechanical properties

The reinforcement mechanism of polymer matrices through the inclusion of particles is a topic of

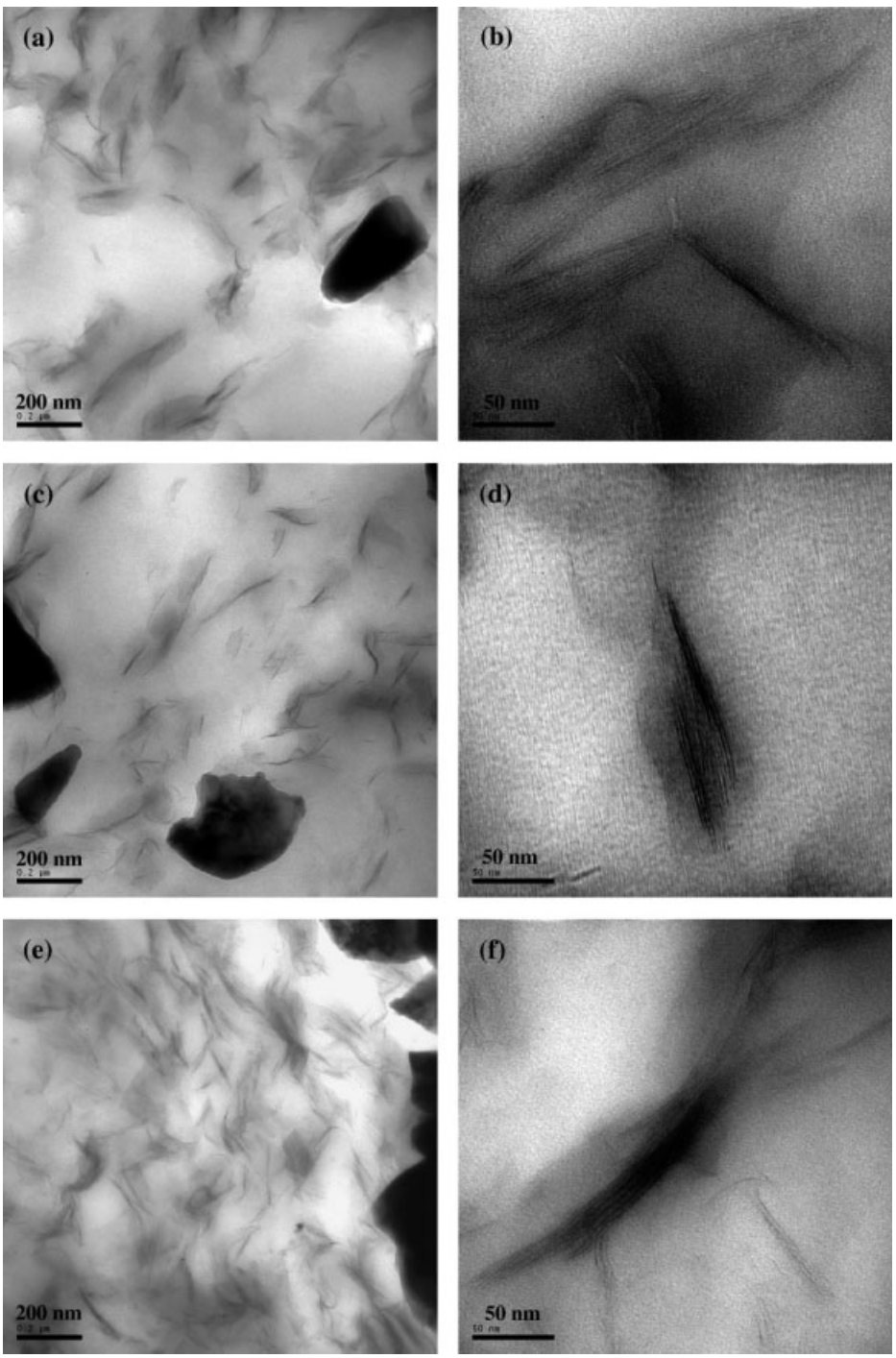

Figure 2 TEM images for the PVC/metallic oxides/O-MMT nanocomposites containing 2.5 wt % O-MMT as a function of metallic oxides content: (a,b) 0, (c,d) 5, and (e,f) 10 wt %.

polymer science that has been widely studied for years. Several authors have agreed that the presence of dispersed particles in the polymer matrix interferes with their mechanical properties, and some models have been developed over the years to correlate the mechanical properties of the pure matrix and reinforcement and the morphology of the obtained composite. Although the initial purpose of these models was to predict the properties of a composite based on its components, these theories allow one to evaluate important parameters, such as modulus reinforcement, volume fraction, aspect ratio, and degree of orientation, and their contribution to the final properties of the composite.

The aspect ratio is an important factor in polymer nanocomposites, and in the case of polymer–clay nanocomposites, it can be defined as the ratio

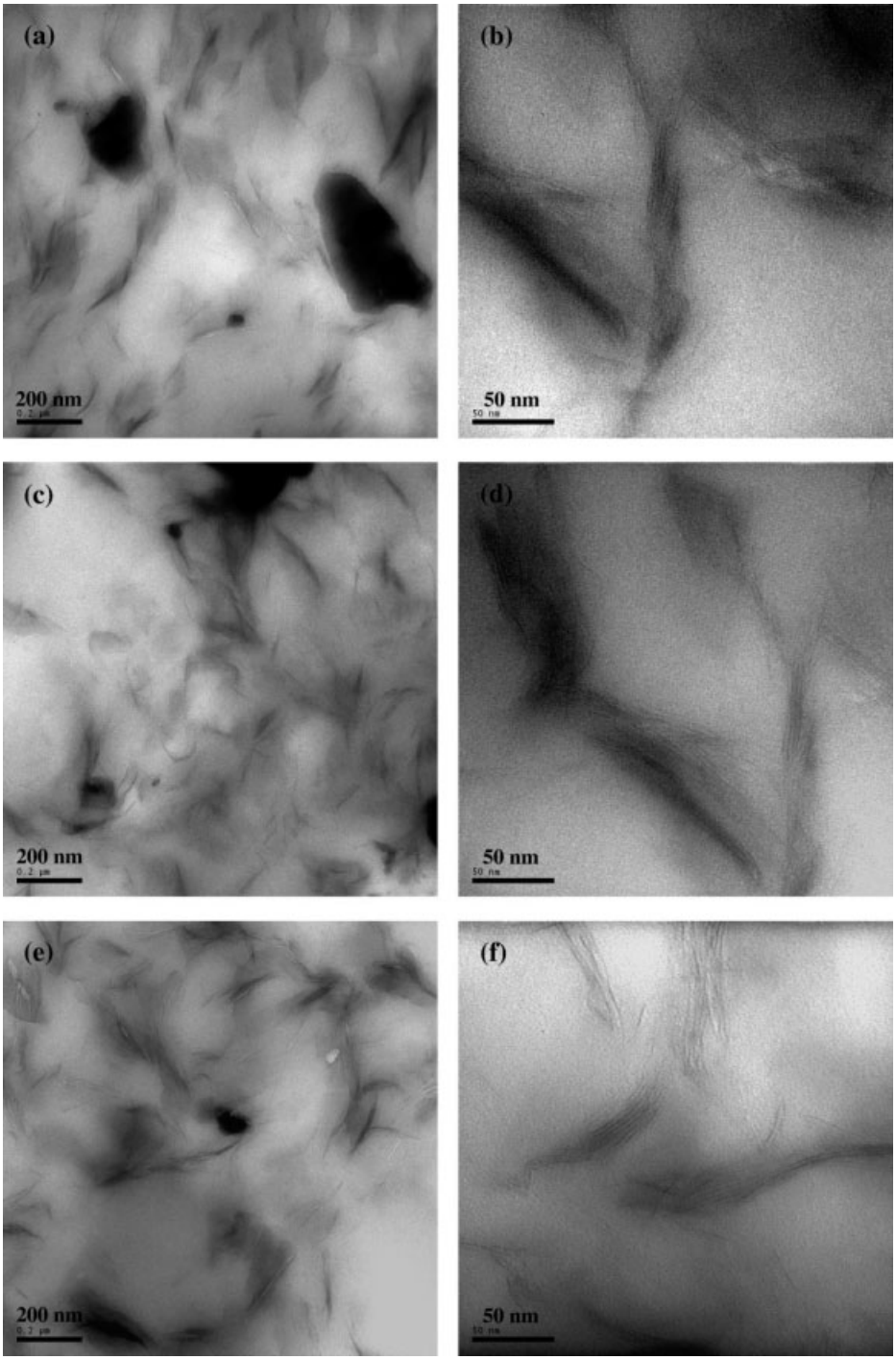

Figure 3 TEM images for the PVC/metallic oxides/O-MMT nanocomposites containing 5 wt % O-MMT as a function of metallic oxides content: (a,b) 0, (c,d) 5, and (e,f) 10 wt %.

between the length of a reinforcement plate and its thickness.

According to the theory developed by Halpin and Tsai, the Young's modulus of a composite can be estimated via the following model:[33]

$$\frac{E}{E_1} = \frac{1 + 2p\eta\phi_2}{1 - \eta\phi_2} \tag{1}$$

$$\eta = \frac{E_r - 1}{E_r + 2p} \tag{2}$$

$$E_r = \frac{E_2}{E_1} \tag{3}$$

where E, E_1, and E_2 correspond to the Young's moduli of the composite, matrix, and reinforcement, respectively; p is the aspect ratio of the

reinforcement; and ϕ_2 is the volume fraction of the reinforcement.

The model presented in eq. (1) is valid for cases in which reinforcement particles are aligned in the direction of the applied stress. In the case of random alignment of the reinforcement particles, an alternative Halpin–Tsai model was developed:[34]

$$\frac{E}{E_1} = \left(\frac{3}{8}\right)\left(\frac{1 + 2p\eta_L\phi_2}{1 - \eta_L\phi_2}\right) + \left(\frac{5}{8}\right)\left(\frac{1 + 2\eta_T\phi_2}{1 - \eta_T\phi_2}\right) \quad (4)$$

where

$$\eta_L = \frac{E_r - 1}{E_r + 2p} \quad (5)$$

$$\eta_T = \frac{E_r - 1}{E_r + 2} \quad (6)$$

Hui and Shia,[35] in turn, developed eq. (7) for the modeling of the Young's modulus of polymer composites that are reinforced with lamellar particles, as in the case treated here:

$$\frac{E}{E_1} = \frac{1}{1 - \frac{\phi_2}{4}\left(\frac{1}{\xi} + \frac{3}{\xi + \Lambda}\right)} \quad (7)$$

where

$$\xi = \phi_2 + \left(\frac{E_1}{E_2 - E_1}\right) + 3(1 - \phi_2)\left[\frac{(1 - g)\alpha^2 - (g/2)}{\alpha^2 - 1}\right] \quad (8)$$

$$\Lambda = (1 - \phi_2)\left[\frac{3(\alpha^2 + 0.25)g - 2\alpha^2}{\alpha^2 - 1}\right] \quad (9)$$

$$g = \frac{\pi}{2}\alpha \quad (10)$$

$$\alpha = \frac{1}{p} \quad (11)$$

Another model developed by Lewis and Nielsen, presented in eq. (12), deals with the Young's modulus of the composite as a function of the maximum packing fraction (ϕ_{max}) of the reinforcement:[36,37]

$$\frac{E}{E_1} = \frac{1 + \omega B\phi_2}{1 - \psi B\phi_2} \quad (12)$$

where

$$\omega = 1.33p^{0.645} \quad (13)$$

$$B = \frac{(E/E_1) - 1}{E/E_1 + \omega} \quad (14)$$

$$\psi = 1 + \frac{1 - \phi_{max}}{\phi_{max}}\phi_2 \quad (15)$$

Values for ϕ_{max} for different particle morphologies can be found in several references in the literature. However, for particles with a high aspect ratio, Sudduth[38] developed a mathematical model for the determination of ϕ_{max} based on the concept of a particle's sphericity (s):

$$\phi_{max} = \left(\frac{0.639}{x - 1}\right)\exp(-0.1334x^4 + 0.9367x^3 - 2.1099x^2 + 0.8507x) \quad (16)$$

where

$$x = s - 1 \quad (17)$$

$$s = \left(\frac{2\alpha + 1}{3\alpha^{2/3}}\right) \quad (18)$$

In this study, values of ϕ_2 were determined for each formulation on the basis of the specific weight values of the nanocomposites, the polymer matrices, and the O-MMT (2.83 g/cm^3).[39,40]

Table III presents a summary of the results for Young's modulus of the PVC/metallic oxides/O-MMT nanocomposites, which are grouped according to the CuO/MoO_3/ZnO content in the PVC matrix. For each situation, we calculated the models considering E_2 = 178 GPa,[39] and the value of the apparent aspect ratio ($\langle p \rangle$) was approximated by the least-squares method. Figure 4 presents the adjustment of the experimental results of the Young's modulus evaluated by different models. The data were well adjusted to the Halpin–Tsai [eq. (1)], random Halpin–Tsai [eq. (4)], and Hui–Shia [eq. (7)] models, as demonstrated both by the adjustment of the points in the graphs of Figure 4 and by the high values for the R^2 correlation coefficient in Table III. The Lewis–Nielsen model [eq. (12)] was not adequately adjusted to the points in any of the three studied situations.

The results show a significant effect of the O-MMT content on the Young's modulus of the nanocomposites, which was expected in the case of the incorporation of high-aspect-ratio reinforcement particles into the polymer matrix.[10–14] When comparing nanocomposites with the same O-MMT content but different metallic oxides contents in the polymer matrix, we observed that the matrices with increasing metallic oxides content had higher Young's modulus values. This happened, even when the effect of the metallic oxides particles themselves, which also had a reinforcing effect, were disregarded because of the physical limitation of the movement of polymer chains in the interface between the matrix and the

TABLE III
Tensile Property Data and Fitting Results ($\langle p \rangle$) for the PVC/Metallic Oxides/O-MMT Nanocomposites as Determined by the Halpin–Tsai, Hui–Shia, and Lewis–Nielsen Models

Formulation	ϕ_2	Young's modulus (MPa)	Stress at break (MPa)	Elongation at break (%)	Halpin-Tsai model [eq. (1)]	Random Halpin–Tsai model [eq. (4)]	Hui–Shia model [eq. (7)]	Lewis–Nielsen model [eq. (12)]
$CuO/MoO_3/ZnO = 0$ wt %								
PVC-0-0	0.000	21.9 ± 1.3	14.0 ± 0.6	48.3 ± 8.8	$\langle p \rangle = 26$	$\langle p \rangle = 68$	$\langle p \rangle = 73$	$\langle p \rangle = 30$
PVC-0-2.5	0.012	33.5 ± 1.3	12.9 ± 0.8	48.8 ± 4.3	$R^2 = 0.9850$	$R^2 = 0.9849$	$R^2 = 0.9828$	$R^2 = 0.9673$
PVC-0-5	0.025	52.4 ± 3.9	10.1 ± 0.4	32.7 ± 9.9				
$CuO/MoO_3/ZnO = 5$ wt %								
PVC-5-0	0.000	20.6 ± 0.8	13.6 ± 0.3	54.5 ± 4.4	$\langle p \rangle = 33$	$\langle p \rangle = 87$	$\langle p \rangle = 94$	$\langle p \rangle = 31$
PVC-5-2.5	0.013	37.2 ± 1.6	12.3 ± 0.4	48.5 ± 4.2	$R^2 = 0.9978$	$R^2 = 0.9978$	$R^2 = 0.9970$	$R^2 = 0.9195$
PVC-5-5	0.026	57.8 ± 3.9	11.7 ± 0.4	38.7 ± 7.3				
$CuO/MoO_3/ZnO = 10$ wt %								
PVC-10-0	0.000	21.6 ± 0.8	12.8 ± 0.4	53.6 ± 5.0	$\langle p \rangle = 39$	$\langle p \rangle = 103$	$\langle p \rangle = 112$	$\langle p \rangle = 31$
PVC-10-2.5	0.013	42.5 ± 2.4	12.2 ± 0.2	41.7 ± 1.2	$R^2 = 0.9970$	$R^2 = 0.9970$	$R^2 = 0.9960$	$R^2 = 0.9130$
PVC-10-5	0.027	69.0 ± 4.9	10.6 ± 0.6	35.5 ± 7.5				

dispersed phase. An examination of the results of Table III shows that, independently of the selected model, the value of $\langle p \rangle$ increased according to the increase in the metallic oxides content in the polymer matrix. A possible explanation for this effect was the possible contribution of metallic oxides particles in the process of exfoliation of the O-MMT during the processing; that is, the metallic oxides particles promoted a milling effect on the piles of silicate lamellae in addition to the shear provided by the processing. The analysis of the experimental results with Design-Expert software showed that the

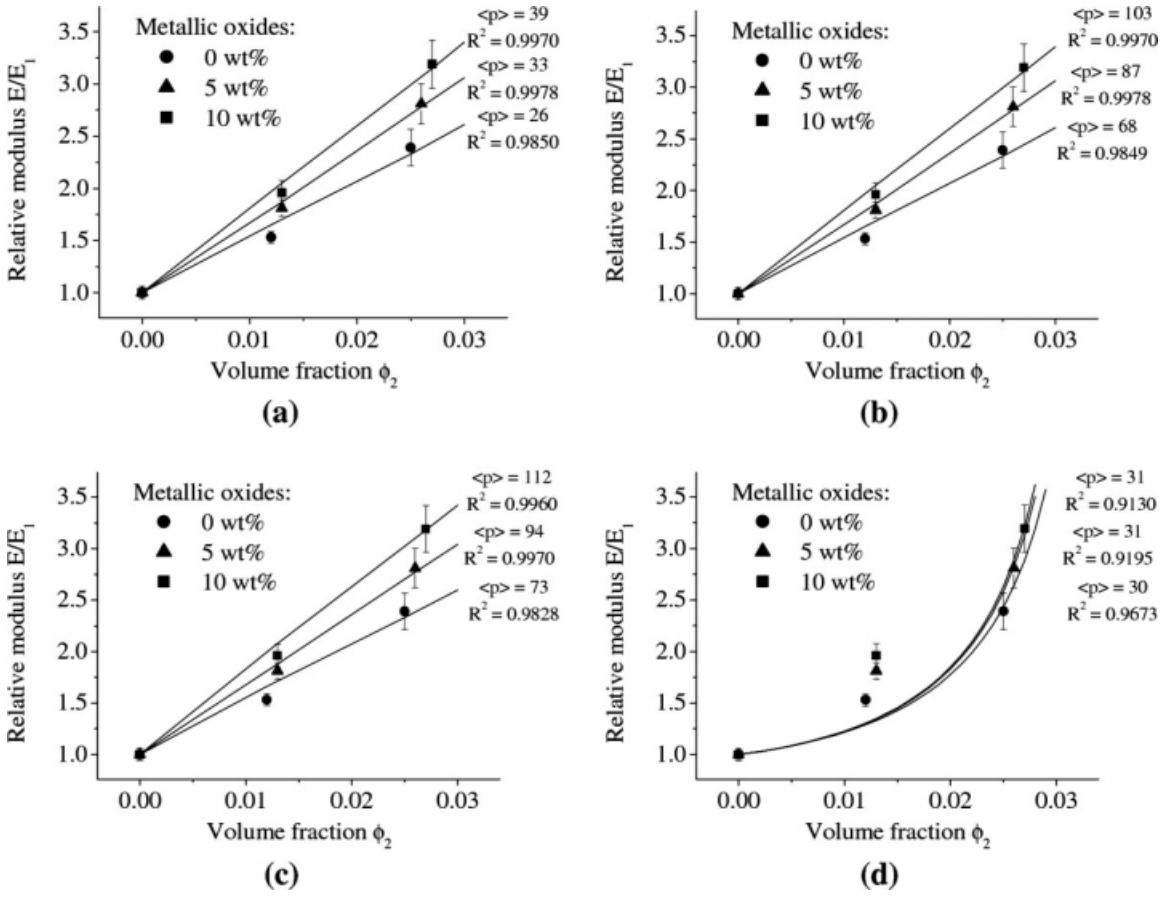

Figure 4 Experimental data and fitting results for PVC/metallic oxides/O-MMT nanocomposites as determined by (a) Halpin–Tsai, (b) random Halpin–Tsai, (c) Hui–Shia, and (d) Lewis–Nielsen models.

TABLE IV
Thermal Property (DMA) Results for the PVC/Metallic Oxides/O-MMT Nanocomposites

Formulation	ϕ_2	Peak E'' (°C)	Peak tan δ (°C)	E' at 23°C (MPa)
$CuO/MoO_3/ZnO$ = 0 wt %				
PVC-0-0	0.000	−17.61	34.96	224.4
PVC-0-2.5	0.012	−16.84	38.23	283.8
PVC-0-5	0.025	−12.89	38.58	341.3
$CuO/MoO_3/ZnO$ = 5 wt %				
PVC-5-0	0.000	−17.21	36.97	225.6
PVC-5-2.5	0.013	−18.38	38.34	312.8
PVC-5-5	0.026	−18.37	44.81	414.3
$CuO/MoO_3/ZnO$ = 10 wt %				
PVC-10-0	0.000	−19.85	35.59	234.1
PVC-10-2.5	0.013	−17.91	39.77	358.8
PVC-10-5	0.027	−8.50	42.02	442.8

effects of the O-MMT content and the metallic oxides content were quite statistically significant, with $p < 0.0001$ and $p = 0.0004$, respectively. As for the stress at break and elongation at break, only the effect of the O-MMT content was statistically significant because the p values were less than 0.0001 and 0.0001, respectively. For the metallic oxides content, the effects on both properties were statistically insignificant, as the p values were equal to 0.2058 and 0.8342, respectively.

The results for the value of $\langle p \rangle$, obtained through the Halpin–Tsai and Lewis–Nielsen models in the nanocomposites obtained in this study were comparable to the values obtained by other researchers. The expected value for the aspect ratio of the O-MMT is a controversial issue in the academic field because some authors[13,14,41] have considered that clays may present aspect ratio values above 1000 when they are fully exfoliated, whereas others, on the basis of TEM image analyses,[12,33,39,42] atomic force microscopy,[43] and rheological measurements,[44,45] have considered values ranging from 50 to 500 for the maximum aspect ratio to be reached by the clay. It is important to highlight the work developed by Ploehn and Liu,[43] who through atomic force microscopy measures in a Na-MMT (Cloisite Na) sample, determined the effective aspect ratio as $p = 166 \pm 86$. By modeling, Borse and Kamal[33] obtained $\langle p \rangle$ values between 10 and 16 (Halpin–Tsai) and 29 and 47 (Hui–Shia) for polyamide 6 nanocomposites with O-MMT (Cloisite 30B) processed by melt blending in a Berstorff ZE 25 twin-screw extruder (screw diameter = 25 mm, length/diameter = 30). In turn, Fornes and Paul[39] obtained $\langle p \rangle$ values between 49 and 57 (TEM image analysis) for polyamide 6 nanocomposites with O-MMT modified with bis(hydroxyethyl) methyl rapeseed quaternary ammonium chloride, also through melt blending, in a twin-screw extruded coupled to a Haake torque rheometer. Even authors who prepared nanocomposites via *in situ* polymerization obtained similar values for $\langle p \rangle$; the modeling of Young's modulus results published by Kojima et al.[46], cited in 13 resulted in $\langle p \rangle$ values of 23 (Halpin–Tsai), 109 (random Halpin–Tsai), and 65 (Hui–Shia), with R^2 ranging between 0.9957 and 0.9959.

Thermal properties

Table IV presents the results of the thermal properties of the PVC/metallic oxides/O-MMT nanocomposites determined through DMA and grouped according to the $CuO/MoO_3/ZnO$ amount in the PVC matrix. We generally observed that the effect of the O-MMT incorporation in the PVC matrix promoted a slight increase in the thermal resistance of the nanocomposite, as the tan δ values increased regardless of the existing metallic oxides content in the nanocomposite. The glass-transition temperature (T_g) values, represented by the temperature in the peak of the loss modulus (E''), also showed a slight increase with increasing O-MMT amount in the nanocomposite. An exception was the series of formulations containing 5 wt % metallic oxides, which showed no significant change in the T_g value with increasing O-MMT content. The analysis of the experimental results with the Minitab software showed that the effect of the O-MMT content in the E'' and tan δ peaks reflected an increment of about 5–6°C in the transition temperatures of the nanocomposites, whereas the effect of the metallic oxides content was practically negligible, as it was not noted in the E'' peak, which represented only an increment of about 2°C in the tan δ peak. The values obtained for the increase in T_g with the formation of the nanocomposites were as high as the results obtained by other researches with the O-MMT and PVC as a polymer matrix.[47–49]

The values of the storage modulus (E'), in turn, confirmed the observations of the modeling

TABLE V
VER and Dynamic Thermal Stability Results for the PVC/Metallic Oxides/O-MMT Nanocomposites

Formulation	VER (10^{13} Ω cm)	Degradation onset time (min)
$CuO/MoO_3/ZnO = 0$ wt %		
PVC-0-0	2.63 ± 0.87	90.4 ± 3.0
PVC-0-2.5	0.120 ± 0.037	8.8 ± 0.8
PVC-0-5	0.0966 ± 0.0022	6.6 ± 0.1
$CuO/MoO_3/ZnO = 5$ wt %		
PVC-5-0	2.50 ± 0.73	7.8 ± 0.6
PVC-5-2.5	0.107 ± 0.027	6.9 ± 0.2
PVC-5-5	0.129 ± 0.022	6.0 ± 0.1
$CuO/MoO_3/ZnO = 10$ wt %		
PVC-10-0	1.70 ± 0.46	6.9 ± 0.3
PVC-10-2.5	0.120 ± 0.022	6.5 ± 0.3
PVC-10-5	0.0312 ± 0.0032	5.3 ± 0.2

performed for the Young's modulus data determined through tensile tests, that is, the formation of partially exfoliated/intercalated nanocomposites and the resulting reinforcement effect of the polymer matrix by the reduction of the molecular mobility due to the presence of platelets with a high aspect ratio.

Electrical properties

Table V presents the results of the VER of the PVC/metallic oxides/O-MMT nanocomposites grouped according to the $CuO/MoO_3/ZnO$ amount in the PVC matrix. The increase in the O-MMT content seemed to have a significant effect on the reduction of the VER values of the nanocomposites. The values of the volumetric resistivity of the O-MMT (between 2.0×10^7 and 3.0×10^7 Ω cm[50,51]) were lower than the value of the volumetric resistivity of the reference PVC compound (2.63×10^{13} Ω cm). Therefore, increasing O-MMT contents in the PVC matrix were expected to reduce the value of VER of the final nanocomposite, even with a simple additive effect considered. The analysis of the experimental results with the Design-Expert software showed that the effect of the O-MMT content was statistically significant, $p < 0.0001$. The effect of the metallic oxide content, in turn, had little significance, with $p = 0.1322$.

Another important factor to be taken into account was the existence of quaternary ammonium salt in the O-MMT, which induced some degree of dehydrochlorination in the PVC matrix and was also harmful to the electrical isolation properties of the obtained nanocomposites.

Dynamic thermal stability

Table V also presents results of the dynamic thermal stability of the PVC/metallic oxide/O-MMT nanocomposites grouped according to the $CuO/MoO_3/ZnO$ content in the PVC matrix.

The analysis of the experimental results with the Design-Expert software showed that the effects of the O-MMT content were statistically significant, $p = 0.0098$. The effect of the metal oxides content was also significant, $p = 0.0099$.

The harmful effects of the quaternary ammonium salt present in O-MMT on the color and thermal stability of PVC nanocomposites have already been widely studied.[49,52] However, in all of the cases in this study, the color and processability were fully satisfactory for the practical application of the obtained nanocomposites. The same was affirmed with respect to the effects of the metallic oxides, particularly in the cases of CuO and ZnO, whose principles of operation for smoke suppression are based on the acceleration of the process of dehydrochlorination of the PVC.[53]

CONCLUSIONS

Flexible PVC nanocomposites, with metallic oxides (copper, molybdenum, and zinc) and O-MMT, were successfully prepared via the process of preexfoliation of the clay in a hot mixture of plasticizers, followed by the intercalation in the molten state (melt blending). Hybrid intercalated/partially exfoliated nanocomposites were obtained in all of the evaluated situations, independently of the metallic oxides content, and this morphology was directly shown by XRD and TEM results and indirectly shown by the significant increase in the Young's modulus of the studied compositions. The modeling of the results of Young's modulus showed that the process of preparation allowed for the effective development of the aspect ratio of the clay, which achieved values that were comparable to those obtained by other researchers for different polymer matrices and processes of preparation of their nanocomposites. The data obtained for the Young's modulus measurements were well adjusted to the Halpin–Tsai, random Halpin–Tsai, and Hui–Shia models; however, the Lewis–Nielsen model was not appropriately adjusted to the points in any of the three studied situations. The effects of the O-MMT content were statistically significant for the Young's modulus, stress at break, and elongation at break of the different observed situations, whereas the metallic oxides particles were credited for an additional milling effect of the O-MMT, which facilitated its exfoliation during the processing. The metallic oxides content did not show statistically significant effects on the stress at break or the elongation at break.

The increase observed in the thermal properties of the nanocomposites was marginal according to the results observed by other researchers who used PVC

as the polymer matrix in their studies. In this case, only the effect of the O-MMT content was statistically significant.

VER measurements showed a significant effect of the O-MMT amount, which caused an important reduction in the electrical insulation properties of the obtained nanocomposites and should be a point of attention when this new class of materials is used where such properties are required or fundamental. Both the O-MMT and metallic oxides contents were significant in the reduction of the dynamic thermal stability of the nanocomposites, according to the reduction of the time needed to achieve the degradation onset in the torque rheometer. In this case, it is worth remarking that despite the reduction of the time needed for the degradation of the nanocomposites, all formulations could be perfectly processed and presented an aspect with very little change in comparison to the reference formulations.

The authors thank Rafael Laurini, Lucas Polito, Max Sakuma, Wilman Terçariol (DMA), Mariele Stocker (TEM), Mauro Oviedo from Braskem S/A, and Charles Dal Castel (XRD) from Universidade Federal do Rio Grande do Sul (UFRGS), whose contributions were fundamental for the completion of this study.

References

1. Smith, M. D. Presented at 2009 World Petrochemical Conference, Houston, TX, March 24–26, 2009.
2. Chow, G.-M.; Kurihara, L. K. In Nanostructured Materials: Processing, Properties and Potential applications; Kock, C. C., Ed.; Noyes: Norwich, New York, 2002.
3. Jordan, J.; Jacob, K. I.; Tannenbaum, R.; Sharaf, M. A.; Jasiuk, I. Mater Sci Eng A 2004, 393, 1.
4. Schmidt, D.; Shah, D.; Giannelis, E. P. Curr Opin Solid State Mater Sci 2002, 6, 205.
5. Yang, F.; Ou, Y.; Yu, Z. J Appl Polym Sci 1998, 69, 355.
6. Gilman, J. W. Appl Clay Sci 1999, 15, 31.
7. Giannelis, E. P. Mater Design 1992, 13, 100.
8. Lan, T.; Kaviratna, P. D.; Pinnavaia, T. J. Chem Mater 1994, 6, 573.
9. Wang, Z.; Lan, T.; Pinnavaia, T. J. Chem Mater 1996, 8, 2200.
10. Alexandre, M.; Dubois, P. Mater Sci Eng R 2000, 28, 1.
11. Ray, S. S.; Okamoto, M. Prog Polym Sci 2003, 28, 1539.
12. Paul, D. R.; Robeson, L. M. Polymer 2008, 49, 3187.
13. Pavlidou, S.; Papaspyrides, C. D. Prog Polym Sci 2008, 33, 1119.
14. Utracki, L. A. Clay-Containing Polymeric Nanocomposites; Rapra Technology: Shropshire, England, 2004; Vol. 1.
15. Rodolfo, A., Jr.; Mei, L. H. I. Polímeros 2007, 17, 263.
16. Wang, D.; Parlow, D.; Yao, Q.; Wilkie, C. A. J Vinyl Additive Technol 2001, 7, 203.
17. Schaefer, D. W.; Justice, R. S. Macromolecules 2007, 40, 8501.
18. Yalcin, B.; Cakmak, M. Polymer 2004, 45, 6623.
19. Kovarova, L.; Kalendova, A.; Gerard, J.-F.; Malac, J.; Simonik, J.; Weiss, Z. Macromol Symp 2005, 221, 105.
20. Benderly, D.; Osorio, F.; Ijdo, W. L. J Vinyl Additive Technol 2008, 14, 155.
21. Rodolfo, A., Jr.; Mei, L. H. I. Polímeros 2009, 19, 1.
22. Peprnicek, T.; Duchet, J.; Kovarova, L.; Malac, J.; Gerard, J.-F.; Simonik, J Polym Degrad Stab 2006, 91, 1855.
23. Peprnicek, T.; Kalendova, A.; Pavlova, E.; Simonik, J.; Duchet, J.; Gerard, J.-F. Polym Degrad Stab 2006, 91, 3322.
24. Francis, N.; Schmidt, D. F. Presented at Annual Technical Conference, May 6–10, 2007, Cincinnati, OH, 2007.
25. Kalendova, A.; Kovarova, L.; Malac, Z.; Malac, J.; Vaculik, J.; Hrncirik, J.; Simonik, J. Presented at Annual Technical Conference, May 5–9, 2002, San Francisco, 2002.
26. Southern Clay Products. Cloisite® 30B—Typical Physical Properties Bulletin. http://www.scprod.com (Accessed July 4, 2009).
27. Faulkner, P. G. J Macromol Sci Phys 1975, 11, 251.
28. Rabinovitch, E. B.; Summers, J. J Vinyl Technol 1980, 2, 165.
29. Marques, R. P.; Covas, J. A. Processing Characteristics of U-PVC Compounds; Companhia Industrial de Resinas Sintéticas: Estarreja, Portugal, 2003.
30. Fillot, L.-A.; Hajji, P.; Gauthier, C.; Masenelli-Varlot, K. J Vinyl Additive Technol 2006, 12, 98.
31. Alves, J. P. D.; Rodolfo, A., Jr. Polímeros 2006, 16, 165.
32. Fornes, T. D.; Yoon, P. J.; Keskkula, H.; Paul, D. R. Polymer 2001, 42, 9929.
33. Borse, N. K.; Kamal, M. R. Polym Eng Sci 2006, 46, 1094.
34. Kim, J. Y.; Han, S. I.; Hong, S. Polymer 2008, 49, 3335.
35. Hui, C. Y.; Shia, D. Polym Eng Sci 1998, 38, 774.
36. Nielsen, L. E.; Landel, R. F. Mechanical Properties of Polymers and Composites, 2nd ed.; CRC: Boca Raton, FL, 1994.
37. Meneghetti, P. C. Ph.D. thesis, Case Western Reserve University, 2005.
38. Sudduth, R. D. Mater Sci Tech 2003, 19, 1181.
39. Fornes, T. D.; Paul, D. R. Polymer 2003, 44, 4993.
40. Ferrigno, T. H. In Handbook of Fillers for Plastics; Katz, H. S.; Milewski, J. V., Eds.; Van Nostrand Reinhold: New York, 1987; Chapter 1.
41. Luo, J.-J.; Daniel, I. M. Compos Sci Technol 2003, 63, 1607.
42. Goettler, L. A. Presented at Annual Technical Conference, May 1–5, 2005, Boston, 2005.
43. Ploehn, H. J.; Liu, C. Ind Eng Chem Res 2006, 45, 7025.
44. Jeon, H. S.; Rameshwaram, J. K.; Kim, G.; Weinkauf, D. H. Polymer 2003, 44, 5749.
45. Rodlert, M.; Plummer, C. J. G.; Leterrier, Y.; Månson, J.-A. E.; Grünbauer, H. J. M. J Rheol 2004, 48, 1049.
46. Kojima, Y.; Usuki, A.; Kawasumi, M.; Okada, A.; Kurauchi, T.; Kamigaito, O. J Appl Polym Sci 1993, 49, 1259.
47. Wan, C.; Qiao, X.; Zhang, Y.; Zhang, Y. Polym Test 2003, 22, 453.
48. Gong, F.; Feng, M.; Zhao, C.; Zhang, S.; Yang, M. Polym Degrad Stab 2004, 84, 289.
49. Awad, W. H.; Beyer, G.; Benderly, D.; Ijdo, W. L.; Songtipya, P.; Jimenez-Gasco, M. M.; Manias, E.; Wilkie, C. A. Polymer 2009, 50, 1857.
50. Manoratne, C. H.; Rajapakse, R. M. G.; Dissanayake, M. A. K. L. Int J Electrochem Sci 2006, 1, 32.
51. Ranaweera, A. U.; Bandara, H. M. N.; Rajapakse, R. M. G. Electrochim Acta 2007, 52, 7203.
52. Wan, C.; Qiao, X.; Zhang, Y.; Zhang, Y. J Appl Polym Sci 2003, 89, 2184.
53. Pike, R. D.; Starnes, W. H., Jr.; Jeng, J. P.; Bryant, W. S.; Kourtesis, P.; Adams, C. W.; Bunge, S. D.; Kang, Y. M.; Kim, A. S.; Kim, J. H.; Macko, J. A.; O'Brien, C. P. Macromolecules 1997, 30, 6957.